IEEE Access
Multidisciplinary | Rapid Review | Open Access Journal

Received October 14, 2018, accepted November 2, 2018, date of publication November 9, 2018,
date of current version January 16, 2019.

Digital Object Identifier 10.1109/ACCESS.2018.2880010

Stochastic Security Assessment for Power Systems With High Renewable Energy Penetration Considering Frequency Regulation

YU HUANG[1], QINGSHAN XU[1], (Member, IEEE), SAJJAD ABEDI[2], (Member, IEEE), TONG ZHANG[3], XIANQIANG JIANG[1], AND GUANG LIN[4], (Member, IEEE)

[1]School of Electrical Engineering, Southeast University, Nanjing 210096, China
[2]School of Mechanical Engineering, Purdue University, West Lafayette, IN 47907, USA
[3]State Grid Jiangsu Electric Power Company Research Institute, Nanjing 211103, China
[4]Department of Mathematics, Purdue University, West Lafayette, IN 47907, USA

Corresponding author: Yu Huang (huangyu@seu.edu.cn)

This work was supported in part by the National Key R&D Program of China under Grant 2016YFB0901100, in part by the Scientific Research Foundation of the Graduate School of Southeast University, and in part by the Postgraduate Research & Practice Innovation Program of Jiangsu Province.

ABSTRACT With the deepening penetration of renewable resources worldwide, power system operators are faced with emerging challenges, e.g., the increase of operating risks due to the volatility and uncertainty of wind and solar power. To efficiently identify the operational limit violations, a switch from deterministic to stochastic framework for assessing the system security, which could manage various types of uncertainties, has been advocated in this paper. The established model is based on an improved probabilistic load flow, which is adapted to incorporate the steady-state behavior of frequency regulation. An efficient importance sampling (IS) technique is also developed to speed up the crude Monte Carlo (MC) simulation in estimating the low probability of violations of security constraints. Extensive computational experiments on both the IEEE 14-bus test case and a simplified regional system show that the proposed IS estimator makes significant enhancement to the crude MC in the computational efficiency and has better numerical performance as compared with other IS schemes.

INDEX TERMS Security risk assessment, numerical method, renewable energy integration, frequency regulation, probability.

I. INTRODUCTION

Operating electric power systems economically and within the security limits has always been a critical and controversial issue for system operators, especially with large-scale integration of renewable energy resources. The combination of market liberalization and additional uncertainty entailed by renewable generation forecast error has significantly increased the operational risk. On the other hand, the electric utilities tend to operate the systems closer to their security margins for more economic gains, which however, could diminish the reliability. To make a trade-off between the reliability and economy, there is a rising need for efficient tools that could give a comprehensive evaluation of the system security level when taking into account various uncertainties [1], [2].

At present, the security assessment tools such as N-1 criterion based methods are mostly deterministic. They are performed under the predefined operating conditions with a given contingency list [3]. The entire system is maintained within adequate security margins to satisfy the worst-case scenario, which may lead to rather conservative results at a higher operational cost far from reality. Therefore, a trend to a new framework for assessing the security of power systems is emerging where stochastic security measurement (SSM) is employed to manage all sorts of uncertainties.

SSM provides a quantitative evaluation of the system security level in terms of the degree and occurrence of violation of technical limits, e.g., transmission line overload and over-/under-voltage violations using probabilistic methods. The risk indices computed, which are dependent on the power flow distribution and uncertainty modeling, are used to enforce an upper bound on each state variable in the optimal power flow (OPF) formulations as reported in [4]. In [5], Wang *et al.* presents a security-constraint stochastic unit commitment (SC-SUC) model by adding security requirements as chance-constraints in case of contingencies.

The transmission line overload probability is evaluated in [6] using the point estimate method accounting for the spatial correlation in the wind-integrated power systems. Security assessment is also performed in [7] to determine the optimal spinning reserve scheduling for the compensation of wind power fluctuations. While the application of SSM is attractive and fundamental, an open question in these literatures is how to conduct the SSM in an accurate and computationally-efficient manner. Towards this end, we take advantage of a powerful tool, i.e., probabilistic load flow (PLF), to calculate the security metrics in the probabilistic framework.

PLF is implemented to capture the steady-state behavior of the highly uncertain systems and can be either solved numerically, e.g., using Monte Carlo simulation (MCS) [8] or analytically. Analytical approaches such as convolution method [9] and cumulant method (CM) [10] are less computationally intensive due to the linearization of power flow equations. The state variables (e.g., node voltage and line flows) could be approximated with acceptable accuracy when following the Gaussian or near-Gaussian distributions. However, the linear and Gaussian assumptions could limit the applicability of the analytical methods especially for more general and complicated practical systems. MCS typically represents the uncertainty by repetitive sampling, and hence it could immune the solution against the model and system restrictions. Nevertheless, the cost of time required for estimating the probability of events with low occurrence (e.g., the violation of operating constraints) could be very high, making it intractable for on-line security computations [11].

To circumvent these problems, in this paper, we propose a novel importance sampling (IS) technique for estimating the very low steady-state operating risks in the presence of renewable resources. The method is in fact a two-stage procedure that, first, modeling of the state variables in the form of piecewise affine approximations, and second, design of an efficient IS estimator based on these approximations. The contributions are threefold summarized as: 1) It comprehensively incorporates the steady-state performance of the frequency regulation in the traditional PLF formulation by considering the dynamic power flow allocation. 2) It can achieve a significant speed-up ratio of MCS by a newly developed IS estimator with numerical robustness and high accuracy. 3) In addition to the security indices such as probability of line overload and voltage violation (as is possible to do with existing methods), it also allows for evaluating the probability of exceeding the ramping capability and probability of violation of over-/under-regulation limits of conventional generators.

The remainder of the paper is organized as follows. In Section II, probabilistic modeling of contingencies and renewable power forecast error is presented. In Section III, we formulate an improved PLF model with the consideration of dynamic power flow allocation and frequency regulation. Section IV presents the methods for constructing the optimal IS estimator. Case studies are performed in Section V where comparisons are made between the proposed IS and other methods. Further discussions and conclusions are made in Section VI and VII.

II. PROBABILISTIC MODELLING OF UNCERTAINTIES

A. MODELLING OF CONTINGENCIES

Contingencies such as outages of lines and generation units could have great impacts on system security, thus should be concerned in the security assessment. Conventionally, generator outage is considered as a discrete random variable represented by the capacity outage probability table (COPT), which gives the probability for each possible capacity level. The line outage in [12] is modeled by two coupled virtual power injections at both ends of the line. This is especially useful as the network structure is kept intact with invariant Jacobi and sensitivity matrices. The equivalent virtual power injections ΔP and ΔQ can be calculated as follows [12].

$$\left[P_{ij}^0, Q_{ij}^0, P_{ji}^0, Q_{ji}^0\right]^{\mathrm{T}} = (\boldsymbol{I}_{4\times4} - \boldsymbol{T}_{4\times4})\left[\Delta P_i, \Delta Q_i, \Delta P_j, \Delta Q_j\right]^{\mathrm{T}} \quad (1)$$

where $\boldsymbol{I}_{4\times4}$ is a 4×4 unity matrix. $\boldsymbol{T}_{4\times4}$ is the sub-matrix of the line flow sensitivity matrix. P_{ij}, Q_{ij} and P_{ji}, Q_{ji} are real and reactive power flows from bus i to j and j to i, respectively. The superscript '0' is for the pre-contingency system.

When the virtual injections ΔP and ΔQ are obtained from Eq. (1), the random line outages could therefore be handled in a similar manner as the random power injections, but with 0-1 distributions given the forced outage rate (FOR) of each line.

B. FORECAST ERROR MODELLING OF LOAD AND RENEWABLE GENERATION

Apart from contingencies, forecast error of load and renewable power is another source of uncertainties that may cause disturbances in the system, and hence raise the security level. The system load L is assumed to be normally distributed in most literature [13], defined as $L \sim N(m_L, \sigma_L)$. The mean value m_L is the point forecast with load forecast error $e_L \sim N(0, \sigma_L)$ around it. Wind and solar power predictions are less accurate than the load forecast, and their error distributions are usually non-Gaussian. The probability density function (PDF) of wind power forecast error is found to be biased and long-tailed [14], and can be modeled by the weighed Beta distribution [14] or other mixed distributions [15]. In [16], a non-parametric approach is used to simulate the forecast error sequence of solar power based on the historical data. Moreover, the methodology in [17] can be used to compute the correlation coefficient matrix [18] to generate the correlated forecast error samples, when given the spatial correlation between the renewable power injections at adjacent nodes.

III. PROBLEM FORMULATION

A. DYNAMIC UNBALANCED POWER ALLOCATION

In the traditional power flow studies, it is assumed that system power imbalance due to the generation-load mismatches is

fully balanced by conventional generators at the slack bus. This assumption may be true for small variations of power injections, but will lead to large deviations from the real operating conditions with increased power uncertainty e.g., renewable generation and flexible load. Dynamic power flow model in [19] shows that the unbalanced power is actually assigned to load and generators that are participating in the control process, where the static frequency regulation characteristics should be taken into account.

The real-time load and renewable power variations can be tracked by the primary and secondary frequency regulation, with which the frequency is maintained within its acceptable limit. With the goal to better coordinate the primary and secondary control, the frequency deviation threshold Δf_T is set that, when the system disturbance is small i.e., $\left|\Delta P_{sys}\right| \leq K_S \Delta f_T$, we consider the mere effect of the primary frequency regulation as

$$\Delta P_{sys} = K_S \Delta f \Rightarrow \Delta f = \Delta P_{sys}/K_S \tag{2}$$

where ΔP_{sys} is the total real power imbalance; K_S is the unit power regulation factor of the system. The frequency deviation Δf can be deduced from Eq. (2).

Accordingly, the unbalanced power allocated to bus i (ΔP_i^b) is given by

$$\begin{aligned} \Delta P_i^b &= \Delta P_{Gi} - \Delta P_{Li} = -K_{Gi}\Delta f - K_{Li}\Delta f \\ &= -\left(K_{Gi} + K_{Li}\right) \Delta P_{sys}/K_S \end{aligned} \tag{3}$$

where K_{Gi}, K_{Li} are the unit power regulation factors of the generator and load at bus i, respectively.

Remark 1: Practically, in order to reduce the frequent action of the controller, we manually set the adjustable dead band Δf_d equal to the average of the dead band of all generator governors in the system. Then the unbalanced power allocation model is modified as

$$\Delta P_i^b = \begin{cases} -K_{Li}\Delta P_{sys}/\sum K_{Li}, & \left|\Delta P_{sys}\right| \leq K_L \Delta f_d \\ -\left(K_{Gi} + K_{Li}\right) \Delta P_{sys}/K_S, & \\ \quad K_L \Delta f_d < \left|\Delta P_{sys}\right| \leq K_S \Delta f_T & \end{cases} \tag{4}$$

When there is a large power imbalance in the system that $\left|\Delta P_{sys}\right| > K_S \Delta f_T$, the total unbalanced power allocated to bus i after the secondary control is calculated as

$$\Delta P_i^b = \alpha_i \Delta P_{sys} \tag{5}$$

where α_i is the participation factor of generator i. This value could be determined according to the use of an affine control strategy [20].

Above all, we finally derive the model of dynamic unbalanced power allocation as

$$\Delta P_i^b = \begin{cases} -K_{Li}\Delta P_{sys}/\sum K_{Li}, & \left|\Delta P_{sys}\right| \leq K_L \Delta f_d \\ -\left(K_{Gi} + K_{Li}\right) \Delta P_{sys}/K_S, & \\ \quad K_L \Delta f_d < \left|\Delta P_{sys}\right| \leq K_S \Delta f_T & \\ \alpha_i \Delta P_{sys}, & \left|\Delta P_{sys}\right| > K_S \Delta f_T \end{cases} \tag{6}$$

Remark 2: For the sake of simplicity, we assume that there are adequate spinning reserves for the primary and secondary regulation, and all dispatched generators are capable of providing the frequency regulation response.

B. PROBABILISTIC LOAD FLOW CONSIDERING FREQUENCY REGULATION

The analytical model in the conventional PLF computation can be expressed in a matrix form as [21]

$$\begin{cases} \Delta \boldsymbol{X} = \boldsymbol{J}_0^{-1} \Delta \boldsymbol{W} = \boldsymbol{S}_0 \Delta \boldsymbol{W} \\ \Delta \boldsymbol{Z} = \boldsymbol{T}_0 \Delta \boldsymbol{W} \end{cases} \tag{7}$$

where $\Delta \boldsymbol{X}$, $\Delta \boldsymbol{Z}$ are state variables, representing the bus voltages and line flows, respectively; $\Delta \boldsymbol{W} = [\Delta \boldsymbol{P} | \Delta \boldsymbol{Q}]$ is the nodal power injections including real and reactive power $\Delta \boldsymbol{P}$ and $\Delta \boldsymbol{Q}$; $\boldsymbol{S_0} = \boldsymbol{J_0^{-1}}$ is the inverse of Jacobian matrix; $\boldsymbol{T}_0$ is the sensitivity matrix of line flows with respect to $\Delta \boldsymbol{W}$.

Due to the consideration of frequency regulation, the unbalanced power allocated to each bus should be added to the nodal power injections, and the first expression in Eq. (7) becomes

$$\Delta \boldsymbol{X} = \left[\boldsymbol{S}_{P0} \,\vdots\, \boldsymbol{S}_{Q0} \right] \begin{bmatrix} \Delta \boldsymbol{P}^{net} + \Delta \boldsymbol{P}^b \\ \hdashline \Delta \boldsymbol{Q}^{net} \end{bmatrix} \tag{8}$$

where $\boldsymbol{S}_{P0}$ and $\boldsymbol{S}_{Q0}$ are the block matrices denoting the real and reactive part of $\boldsymbol{S}_0$. The superscript 'net' highlights the net increase of power injections before the frequency control, and is omitted for simplicity in the rest of the paper. For an n-bus network, $\Delta \boldsymbol{P}^b = \left[\Delta P_1^b, \cdots, \Delta P_i^b, \cdots \Delta P_n^b\right]^T$ is the vector of the unbalanced power allocated to each node. The reactive power injections are kept unchanged because of the weak coupling with the frequency. Substituting Eq. (6) into Eq. (8), we obtain the piecewise linearized form of $\Delta \boldsymbol{X}$ in the following three segment ($\left|\Delta P_{sys}\right| \leq K_L \Delta f_d$, $K_L \Delta f_d \leq \left|\Delta P_{sys}\right| \leq K_S \Delta f_T$ and $\left|\Delta P_{sys}\right| > K_S \Delta f_T$) as

$$\Delta \boldsymbol{X} = \begin{cases} \boldsymbol{S}_{P0} \left(\Delta \boldsymbol{P} - \boldsymbol{K}_L \Delta P_{sys}/\sum K_{Li} \right) + \boldsymbol{S}_{Q0} \Delta \boldsymbol{Q} \\ \boldsymbol{S}_{P0} \left[\Delta \boldsymbol{P} - \left(\boldsymbol{K}_G + \boldsymbol{K}_L \right) \Delta P_{sys}/K_S \right] + \boldsymbol{S}_{Q0} \Delta \boldsymbol{Q} \\ \boldsymbol{S}_{P0} \left(\Delta \boldsymbol{P} + \boldsymbol{\alpha} \Delta P_{sys} \right) + \boldsymbol{S}_{Q0} \Delta \boldsymbol{Q}, \end{cases} \tag{9}$$

where $\boldsymbol{K}_G = [K_{G1}, K_{G2}, \cdots, K_{Gn}]^T$; $\boldsymbol{K}_L = [K_{L1}, K_{L2}, \cdots, K_{Ln}]^T$ and $\boldsymbol{\alpha} = [\alpha_1, \alpha_2, \cdots, \alpha_n]^T$.

$$\Delta P_{sys} \approx \sum_{i=1}^{n} \left(\Delta P_{Gi} + \Delta P_{Ri} + \Delta P_{Ci} - \Delta P_{Li} \right) = \sum_{i=1}^{n} \Delta P_i \tag{10}$$

where ΔP_{Gi}, ΔP_{Ri}, ΔP_{Ci} and ΔP_{Li} are the incremental power injections at bus i with respect to the conventional generators, renewable resources, contingencies and load, respectively.

If we define $H(\boldsymbol{\alpha}) = \begin{bmatrix} 1+\alpha_1 & \alpha_1 & \cdots & \alpha_1 \\ \alpha_2 & 1+\alpha_2 & \cdots & \alpha_2 \\ \vdots & \vdots & \ddots & \vdots \\ \alpha_n & \alpha_n & \cdots & 1+\alpha_n \end{bmatrix}$, then Eq. (9) can be rewritten as

$$\Delta \boldsymbol{X} = \begin{cases} \boldsymbol{S}_{P0} H\left(-\boldsymbol{K}_L / \sum K_{Li}\right) \Delta \boldsymbol{P} + \boldsymbol{S}_{Q0} \Delta \boldsymbol{Q} \\ \boldsymbol{S}_{P0} H\left[-(\boldsymbol{K}_G + \boldsymbol{K}_L)/K_S\right] \Delta \boldsymbol{P} + \boldsymbol{S}_{Q0} \Delta \boldsymbol{Q} \\ \boldsymbol{S}_{P0} H(\boldsymbol{\alpha}) \Delta \boldsymbol{P} + \boldsymbol{S}_{Q0} \Delta \boldsymbol{Q} \end{cases} \tag{11}$$

Given that the load flow equation is linearized around a specific point (normal operating point), the deviations that are far away from this point may cause significant truncated errors, especially in the process of secondary control. Herein, we present a multi-linearization scheme to improve the accuracy of the single-point linearization.

When $\left|\Delta P_{sys}\right| > K_S \Delta f_T$, we firstly divide the system unbalanced power into m even intervals (i.e., $\left[\Delta P^0_{sys}, \Delta P^1_{sys}\right], \ldots, \left[\Delta P^{m-1}_{sys}, \Delta P^m_{sys}\right]$). The integer m should be properly selected according to the scale of ΔP_{sys}. Suppose that $\mu_1, \cdots, \mu_m$ are the mean values of the each interval, the linearization point of the kth interval $\left[\boldsymbol{P}_k | \boldsymbol{Q}_k\right]^T$ can be determined as

$$\begin{bmatrix} \boldsymbol{P}_k \\ \text{----} \\ \boldsymbol{Q}_k \end{bmatrix} = \begin{bmatrix} \boldsymbol{P}_0 \\ \text{----} \\ \boldsymbol{Q}_0 \end{bmatrix} + \mu_k \begin{bmatrix} \boldsymbol{\alpha} \\ \text{----} \\ \boldsymbol{0} \end{bmatrix}, \quad k = 1, 2 \cdots, m \tag{12}$$

where '$\boldsymbol{0}$' is a $n \times 1$ zero vector. Then the mathematical expression corresponding to the steady-state performance of the secondary control (the third expression in Eq. (11)) can be modified as

$$\Delta \boldsymbol{X} = \boldsymbol{S}_{P_k} H(\boldsymbol{\alpha}) \Delta \boldsymbol{P}' + \boldsymbol{S}_{Q_k} \Delta \boldsymbol{Q}', \quad k = 1, 2, \cdots, m \tag{13}$$

where $\boldsymbol{S}_k = \left[\boldsymbol{S}_{Pk} | \boldsymbol{S}_{Qk}\right]^T$ is the inverse of Jacobian matrix with respect to the linearization point in the kth interval. $\boldsymbol{P}'$ and $\boldsymbol{Q}'$ are the net power injections corresponding to the new linearization point $\boldsymbol{S}_k$.

Similarly, we can also have a modified model for the line flows $\boldsymbol{Z}$ in a piecewise linear form as Eq. (11) to incorporate the steady-state performance of frequency regulation.

Remark 3: Although the multi-linearization process can extend the linear model to handle the input variables with large variations, the errors are likely to be ignored under the following circumstances: 1) The equivalent power injections of line outages are much larger than those of the load and renewable generation. 2) The nodal power injections are large but with opposite directions and offset each other. To address these issues, we alternatively use the conventional Newton iteration method to obtain more precise results in case that the variation of voltage angle $|\Delta\theta|$ (calculated via Eq. (11) and (13)) exceeds a predefined threshold ΔC_T.

IV. IMPORTANTANCE SAMPLING FOR SECURITY ASSESSMENT

A. CHALLENGES FOR MONTE CARLO SIMULATION

The main task in the stochastic security assessment is to compute the probabilities of violating the security constraints, which in essence is a rare-event simulation problem, defined as

$$\mu = \mathrm{E}\left[\mathbf{1}\{X > c\}\right] \tag{14}$$

where c is a predefined threshold; $\mathbf{1}\{\cdot\}$ is an indicator function for the random variable X. μ can be estimated numerically by performing MCS as follows.

$$\hat{\mu} = \frac{1}{N} \sum_{i=1}^{N} \mathbf{1}\left\{X^i > c\right\} \tag{15}$$

where $X^i (i = 1, 2, \cdots, N)$ are the random samples of X. As for the case in section III, X is the state variable expressed as a piecewise affine function of input power injections, for which the PDFs are known and can be sampled directly.

The accuracy of MCS estimate can be measured by w_d, called the relative half-width of 95% confidence interval. According to the Central Limit Theorem [22], the confidence interval for any random variable at 95% probability should be within the interval $\left[\mu \pm 1.96\sigma/\sqrt{N}\right]$ when the sample size N is large enough. We could thus obtain the width as

$$w_d = 1.96 \frac{\sigma}{\mu\sqrt{N}} \tag{16}$$

For a given w_d, the number of MCS is demanded as

$$N(w_d, \sigma) = 1.96^2 \frac{\sigma^2}{w_d^2 \mu} \tag{17}$$

Note that $\mathbf{1}\{X > c\}$ is actually a Bernoulli random variable with success probability μ and the variance $\sigma^2 = \mu(1-\mu)$. If μ is very small, Eq. (17) can be simplified as

$$N = 1.96^2 \frac{\mu(1-\mu)}{w_d^2 \mu^2} \approx 1.96^2 \frac{1}{w_d^2 \mu} \tag{18}$$

For probabilities of order 10^{-4} with $w_d = 0.1$, it requires running the simulation for more than one million times, which is considerably time-consuming. A method for reducing this computational challenge is presented in the following sections.

B. IMPORTANCE SAMPLING TECHNIQUE

As can be seen in Eq. (17), the required MCS runs are dependent on the variance σ^2. Therefore, the speed-up of MCS can be achieved by the variance reduction technique and importance sampling (IS) is considered in this paper.

The IS is originally used in the portfolio risk management [23] for estimating the probability of investment losses and can be adapted to other rare-event simulations. It makes the use of the measure transformation to allow more samples

that are generated from a new distribution (measure) to be within a certain collection of the indicator function.

$$\mu = \mathrm{E}\left[\mathbf{1}\left\{X > c\right\}\right] = \mathrm{E}_g\left[\mathbf{1}\left\{X > c\right\}\frac{f\left(X\right)}{g\left(X\right)}\right] \tag{19}$$

where $g(\cdot)$ is the IS distribution developed to acquire higher probabilities of the out-of-limit events; $E_g(\cdot)$ is the expectation with respect to g; The term $f(X)/g(X)$ is called the likelihood ratio, denoted as $l(X)$. We could obtain μ with an IS estimator as

$$\hat{\mu} = \frac{1}{N}\sum_{i=1}^{N}\mathbf{1}\left\{\tilde{X}^i > c\right\} l\left(\tilde{X}^i\right) \tag{20}$$

where $\tilde{X}^i$ are samples drawn from g. The variance σ^2 in Eq. (17) now becomes $\tilde{\sigma}^2$ (the variance of $\mathbf{1}\{X > c\}l(X)$ under g), hence the computational efficiency could be enhanced using IS provided $\tilde{\sigma} < \sigma$.

C. ALGORITHMS FOR FINDING OPTIMAL IMPORTANCE SAMPLING DISTRIBUTION

Given the salient feature of IS, a question that arises naturally is how to design an efficient IS estimator. In [24], a two-step method for computing the IS distribution in mathematical finance is presented which is also adaptable to our application.

Step 1: Modify the approximation of state variables evaluated in the system. The input power injections $\Delta \boldsymbol{W}$ in Eq. (11) with arbitrary distributions must be modified to be readily utilized by the IS technique. Firstly, ΔW_i is expressed by the intermediate variable V_i as

$$\Delta W_i = F_i^{-1}\left[\Phi\left(V_i\right)\right], \quad i = 1, 2, \cdots, n \tag{21}$$

where $V_i \sim N(0, 1)$ is the standard normal variable; $F_i(\cdot)$ and $\Phi(\cdot)$ are cumulative distribution functions (CDFs) of ΔW_i and V_i, respectively. $F_i^{-1}(\cdot)$ is the inverse function of ΔW_i.

To guarantee the desired correlation of $\Delta \boldsymbol{W}$ at different nodes, the correlation coefficient matrix $\boldsymbol{R}_V$ of $\boldsymbol{V}$ should be determined empirically as in [25]. Let $\boldsymbol{R}_V = \boldsymbol{L}\boldsymbol{L}^T$ be the Cholesky decomposition of $\boldsymbol{R}_V$, where $\boldsymbol{L}$ is the lower triangular matrix. Suppose that $\boldsymbol{Z} = [Z_1, Z_2, \cdots, Z_n]^T$ is the uncorrelated normal vector, we have

$$\boldsymbol{Z} = \boldsymbol{L}^{-1}\boldsymbol{V} \tag{22}$$

Once the explicit expression between $\Delta \boldsymbol{W}$ and $\boldsymbol{Z}$ is obtained, the state variable X can be approximated as a function of $\boldsymbol{Z}$, which fulfills the prerequisite of the IS implementation. The above process is the so-called Nataf transformation that allows for the mapping of the correlated random variables in their original space into the uncorrelated standard normal domain.

Step 2: Find the optimal IS distributions for estimating the probability of violations. Suppose that $\boldsymbol{Z} \sim N(\boldsymbol{\theta}, \boldsymbol{I}_n)$ is shifted from the original standard normal PDF $\Phi(\cdot)$ after the measure transformation, then the likelihood ratio l and probability μ are respectively given as

$$l\left(\boldsymbol{Z}\right) = \frac{\Phi\left(\boldsymbol{Z}\right)}{\Phi^{\theta}\left(\boldsymbol{Z}\right)} = \exp\left(-\boldsymbol{\theta}^{\mathrm{T}}\boldsymbol{Z} + \frac{1}{2}\boldsymbol{\theta}^{\mathrm{T}}\boldsymbol{\theta}\right) \tag{23}$$

$$\begin{aligned}\mu &= P\left\{X\left(\boldsymbol{Z}\right) > c\right\} = \mathrm{E}\left[\mathbf{1}\left\{X\left(\boldsymbol{Z}\right) > c\right\}\right] \\ &= \mathrm{E}_{\Phi^{\theta}}\left[\mathbf{1}\left\{X\left(\boldsymbol{Z}\right) > c\right\}\exp\left(-\boldsymbol{\theta}^{\mathrm{T}}\boldsymbol{Z} + \frac{1}{2}\boldsymbol{\theta}^{\mathrm{T}}\boldsymbol{\theta}\right)\right]\end{aligned} \tag{24}$$

where $\boldsymbol{\theta}$ is the shifting parameter that dominates the performance of an IS estimator; Φ^{θ} is the desired IS distribution from which the samples $\tilde{Z}^i$ are drawn for estimating the approximation of μ.

$$\hat{\mu} = \frac{1}{N}\sum_{i=1}^{N}\mathbf{1}\left\{X\left(\tilde{Z}^i\right) > c\right\}\exp\left(-\boldsymbol{\theta}^{\mathrm{T}}\tilde{\boldsymbol{Z}}^i + \frac{1}{2}\boldsymbol{\theta}^{\mathrm{T}}\boldsymbol{\theta}\right) \tag{25}$$

The optimal $\boldsymbol{\theta}$ selected is the one that gives the minimum variance of μ in Eq. (24). Since IS is an unbiased estimator, the variance reduction of μ is equivalent to the decrease of its second-order moment as

$$\begin{aligned}&\mathrm{E}_{\Phi^{\theta}}\left[\mathbf{1}\left\{X\left(\boldsymbol{Z}\right) > c\right\} l^2\left(\boldsymbol{Z}\right)\right] \\ &= \mathrm{E}_{\Phi^{\theta}}\left[\mathbf{1}\left\{X\left(\boldsymbol{Z}\right) > c\right\}\exp\left(-2\boldsymbol{\theta}^{\mathrm{T}}\boldsymbol{Z} + \boldsymbol{\theta}^{\mathrm{T}}\boldsymbol{\theta}\right)\right] \\ &= \mathrm{E}\left[\mathbf{1}\left\{X\left(\boldsymbol{Z}\right) > c\right\}\exp\left(-\boldsymbol{\theta}^{\mathrm{T}}\boldsymbol{Z} + \frac{1}{2}\boldsymbol{\theta}^{\mathrm{T}}\boldsymbol{\theta}\right)\right]\end{aligned} \tag{26}$$

Consequently, the optimal shifting point $\boldsymbol{\theta}^*$ is determined by a generalized stochastic optimization problem as

$$\begin{aligned}\boldsymbol{\theta}^* &= \arg\min f\left(\boldsymbol{\theta}\right) \\ &= \arg\min_{\boldsymbol{\theta}} \mathrm{E}\left[\mathbf{1}\left\{X\left(\boldsymbol{Z}\right) > c\right\}\exp\left(-\boldsymbol{\theta}^{\mathrm{T}}\boldsymbol{Z} + \frac{1}{2}\boldsymbol{\theta}^{\mathrm{T}}\boldsymbol{\theta}\right)\right]\end{aligned} \tag{27}$$

The Eq. (27) can be numerically solved by ***Newton*** method [26]. We use the first and second derivatives of $f(\theta)$ (gradient $\nabla f(\boldsymbol{\theta})$ and Hessian matrix $\nabla^2 f(\boldsymbol{\theta})$) to construct an iterative format of $\boldsymbol{\theta}$. The major challenges include the estimates of $\nabla f(\boldsymbol{\theta})$, $\nabla^2 f(\boldsymbol{\theta})$ at each iteration and the inverse operation for the high order of Hessian matrix. In [27], Glasserman simplified the problem Eq. (27) by substituting the expectation on the right-hand side with the ***Laplace*** estimate based on large deviation theorem. Computational gains could be achieved as no iteration is needed compared with Newton method, but its numerical stability needs to be further examined.

Herein, we present a new way of solving Eq. (27) as follows. The optimal solution $\boldsymbol{\theta}^*$ must satisfy that $\nabla f(\boldsymbol{\theta}^*) = 0$, which can be written as

$$\begin{aligned}&\mathrm{E}\left[-\mathbf{1}\left\{X\left(\boldsymbol{Z}\right) > c\right\}\exp\left(-\boldsymbol{\theta}^{*\mathrm{T}}\boldsymbol{Z} + \frac{1}{2}\boldsymbol{\theta}^{*\mathrm{T}}\boldsymbol{\theta}^*\right)\boldsymbol{Z}\right] \\ &\quad + \mathrm{E}\left[\mathbf{1}\left\{X\left(\boldsymbol{Z}\right) > c\right\}\exp\left(-\boldsymbol{\theta}^{*\mathrm{T}}\boldsymbol{Z} + \frac{1}{2}\boldsymbol{\theta}^{*\mathrm{T}}\boldsymbol{\theta}^*\right)\boldsymbol{\theta}^*\right] = 0\end{aligned} \tag{28}$$

If the stochastic term $\exp(-\boldsymbol{\theta}^{*T}\boldsymbol{Z})$ in the expectation operator is regarded as a constant, the common item

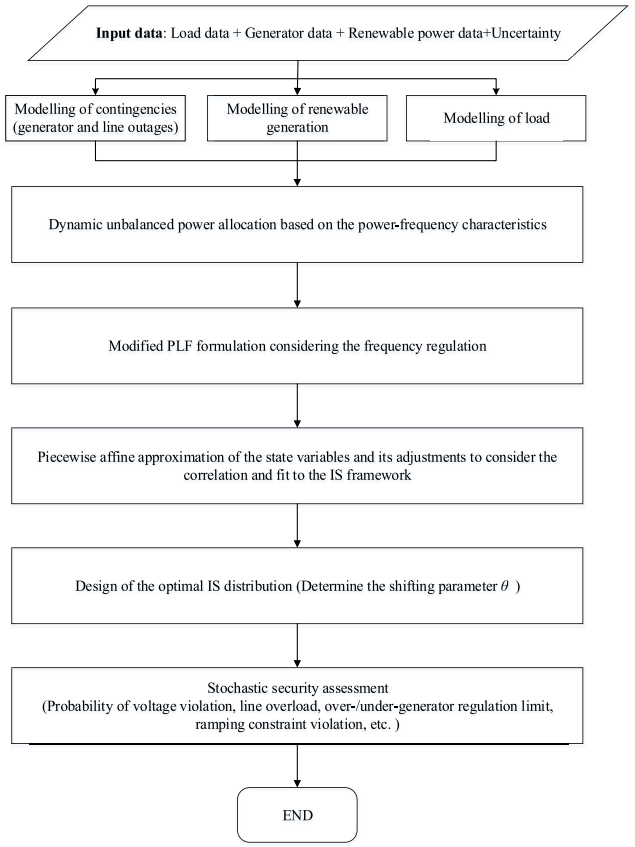

FIGURE 1. Flowchart of the proposed stochastic security assessment.

$\exp(-\boldsymbol{\theta}^{*T}\boldsymbol{Z} + \frac{1}{2}\boldsymbol{\theta}^{*T}\boldsymbol{\theta}^{*})$ in the first and second expectation operators can be divided out, which yields

$$\tilde{\boldsymbol{\theta}}^{*} = \frac{\mathrm{E}\left[\mathbf{1}\left\{X\left(\mathbf{Z}\right) > c\right\}\mathbf{Z}\right]}{\mathrm{E}\left[\mathbf{1}\left\{X\left(\mathbf{Z}\right) > c\right\}\right]} \tag{29}$$

where $\tilde{\boldsymbol{\theta}}^{*}$ is asymptotically optimal for $\boldsymbol{\theta}^{*}$, and could be estimated by MCS. It is evident that the proposed algorithm is very simple and easy to implement. Detailed information regarding its accuracy and numerical stability will be tested and discussed in the next section.

Fig. 1 depicts the flowchart of conducting the proposed approach to the stochastic security assessment using the IS scheme based on a modified PLF model which incorporates the steady-state behavior of the frequency regulation.

V. CASE STUDIES

Two case studies are carried out to evaluate the performance of the proposed methodology: the modified IEEE 14-bus system and a simplified regional power system in the east coast of China. We focus on assessing the system security level in a look-ahead horizon with datasets of renewable energy, load production and their forecasts. The improved PLF model and its adapted sampling techniques are implemented using Matlab 2014b on a PC with Intel core i5 3.0 GHz and 3GB of RAM.

TABLE 1. Parameters of wind power forecast error.

Bus	a_k	b_k	R_W
12	25	25	$\begin{bmatrix} 1 & 0.6 \\ 0.6 & 1 \end{bmatrix}$
13	34	36	

A. MODIFIED 14-BUS SYSTEM

The network configuration and data used in the base case of IEEE 14-bus system can be referred to [28]. Two wind farms are installed at nodes 12 and 13 with forecasted power of 20 MW and 30 MW at time t_k, respectively. The forecast error for wind power is modeled by Beta distribution $\beta_k(a_k, b_k)$ as in [24], the parameters of which are given in table 1 and the correlation coefficient between them is 0.6. The load forecasts at t_k are assumed to be equal to their base values and the uncertainty is represented as 10% deviation from their forecasts. In this system, generators at bus 1 ($g1$) and 2 ($g2$) play the role of sharing the power imbalance based on their participation factors ($\alpha_1 = 0.55$, $\alpha_2 = 0.45$), whereas the other generators are functioned as synchronous compensators. The assumed FORs representing random outages of $g1$, $g2$ and all lines are 1.12%, 1.34% and 0.15%, respectively. Other associated parameters are set as $K_{G1} = 25$, $K_{G2} = 15$, $G_L = 1.5$, $\Delta f_d = 0.005Hz$, $\Delta f_T = 0.1Hz$, $\Delta C_T = 0.1rad$.

The estimates of probabilities of voltage violations and line overloads using the proposed IS are compared to those obtained by crude Monte Carlo (MC) in table 2 for four specific examples (V_{10}, V_{14}, P_{3-4} and P_{12-13}). Two scenarios are conducted with and without the consideration of the frequency regulation. Each $\hat{\mu}$ is the average of five repetitive simulations. The required number of samples for the two sampling techniques to reach $w_d = 0.1$ are shown in columns 3 and 6, and their ratio r (speed-up ratio) demonstrates the enhancement of the computational efficiency.

It can be seen that for a predefined accuracy level, the proposed IS scheme could reduce the necessary MC runs from up to ten thousand to only a few hundred times, which is significantly more efficient than the crude MC method. It is also worth noting that for smaller probabilities as in the case of V_{10} and P_{3-4}, larger gains could be achieved with the ratio up to order of 10^2. Conversely, when estimating higher operating risks (e.g. $\hat{\mu} = 0.024$ for P_{12-13}). Since the occurrence of violations is not that rare, the speed-up effect is less obvious. Moreover, results between the two scenarios show a non-negligible difference, which is relatively subtle for the bus voltage, but profound when it turns to line flows. As for the examples of V_{10} and P_{12-13} whose CDFs are illustrated in Fig. 2, we can see that the range of variations in both cases get reduced when not considering the frequency regulation, which in turn, may result in the underestimation of the system risk level.

Our security assessment model also allows for evaluating the probabilities of violating the under-/over-regulation limits

TABLE 2. Comparisons of Crude MC and the proposed IS in estimating the probabilities of voltage violations and line overloads with and without frequency control in the IEEE 14-bus system.

	With Frequency Control			Without Frequency Control		
	$\hat{\mu}$	N^0_{CMC} / N^0_{IS}	r	$\hat{\mu}$	N^0_{CMC} / N^0_{IS}	r
V_{10}	3.2×10^{-3}	120000 / 680	176	3×10^{-3}	128000 / 680	188
V_{14}	8.2×10^{-3}	46800 / 650	72	7.6×10^{-3}	50500 / 650	78
$P_{3\text{-}4}$	3.8×10^{-3}	101000 / 660	153	3.2×10^{-4}	651000 / 790	824
$P_{12\text{-}13}$	0.024	16000 / 590	27	0.018	21300 / 600	36

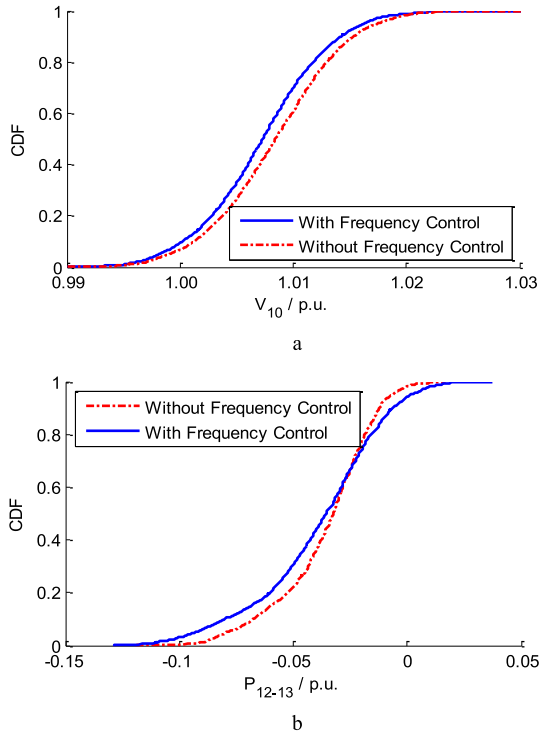

FIGURE 2. CDF comparison of the bus voltage and line flow with and without considering the frequency control: (a) V_{10}, (b) P_{12-13}.

of dispatched generators. Suppose that the tolerance band of generator $g1$ and $g2$ are [0.4, 3.0] p.u. and [0.2, 0.6] p.u., respectively. The output of $g1$ and $g2$ (denoted by $\tilde{P}_{g1}$ and $\tilde{P}_{g2}$) considering the process of unbalanced power allocation is given as

$$\tilde{P}_{g_i} = \bar{P}_{g_i} + \Delta P_i^b, \quad i = 1, 2 \tag{30}$$

where $\bar{P}_{g_i}$ is the expected value of $\tilde{P}_{g_i}$ obtained by traditional power flows without frequency regulation; The expression of the unbalanced power ΔP_i^b is given by Eq. (6).

To confirm the effectiveness of the proposed IS scheme on the computational performance, we comparatively tested the aforementioned three IS methods in section IV.C (denoted as

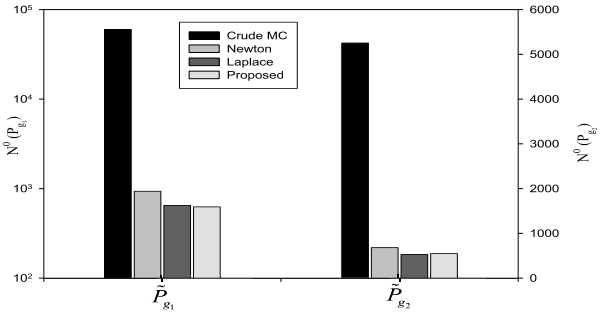

FIGURE 3. Number of samples needed to achieve the accuracy level of $w_d = 0.5$ using crude MC and different IS schemes.

Newton, Laplace and Proposed for short) with crude MC as a reference. Fig. 3 shows the number of samples N^0 needed for reaching the accuracy level of $w_d = 0.5$ (Note the logarithmic scale on the left-hand y-axis for $\tilde{P}_{g1}$). Significant reduction in MC runs can be observed in both cases using one of the IS schemes, among which the Laplace and Proposed have similar order of magnitude of the speed-up ratio, while the Newton is outperformed by them demanding a few more simulations. The big gap in the number of samples required by the crude MC for $\tilde{P}_{g1}$ and $\tilde{P}_{g2}$ due to the different security level turns out to be obscure when using IS methods.

For detailed comparisons among the three IS schemes in terms of both the computational accuracy and numerical robustness, the relative error index in Eq. (31) is adopted to demonstrate the degree of deviation for the estimated probabilities of $\tilde{P}_{g1}$ and $\tilde{P}_{g2}$ versus the sample size $N = 200, 300, \cdots, 1000$ as shown in Fig. 4.

$$\varepsilon_\mu^\gamma = \left| \frac{\hat{\mu}_{IS} - \mu^t}{\mu^t} \right| \times 100\% \tag{31}$$

where ε_μ^γ is the average error of probability μ with superscript γ referring to the specific state variables. $\hat{\mu}_{IS}$ and μ^t are the IS estimate and the true value of μ (obtained by 100000 MCS), respectively.

We can see from Fig. 4 that the Laplace and Proposed give consistently more accurate results than the Newton for the same sample size from 200 to 1000. The relative error of Newton is extremely large with less than 200 samples, after which it drops rapidly before leveling out when $N > 800$. In contrast, the error curves of either the Laplace or Proposed is steadier and remain almost stationary after 600 samples, indicating numerical robustness and good convergence property. Despite of a significant difference in the initial errors between $\tilde{P}_{g1}$ and $\tilde{P}_{g2}$ ($N = 200$), the accuracy of the three methods could finally reach the same order of magnitude with sufficient samples.

B. SIMPLIFIED REAL REGIONAL SYSTEM

The performance and feasibility of the proposed method is further tested on a larger and actual system here: the simplified real regional system in east part of China with data collected from Jiangsu Electric Power Dispatching

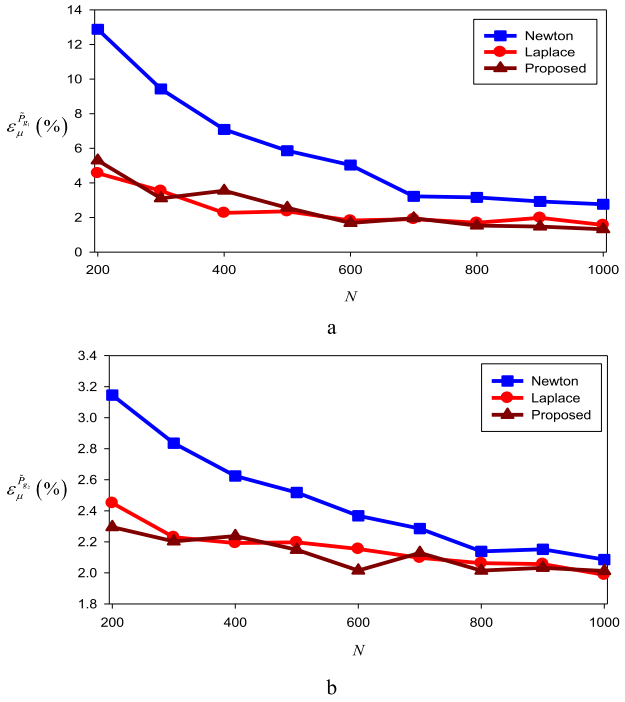

FIGURE 4. Error curve comparisons of $\tilde{P}_{g1}$ and $\tilde{P}_{g2}$ by different IS schemes in the IEEE 14-bus system: (a) $\tilde{P}_{g1}$, (b) $\tilde{P}_{g2}$.

TABLE 3. Parameters for 6 wind farms in the regional power grid at time steps t_k and t_{k+1}.

Bus	a_k	b_k	a_{k+1}	b_{k+1}	R_W	P_k	P_{k+1}
12	35	35	36	38		16.8	32.3
18	28	28	28	28	$\begin{bmatrix} 1 & 0.2 & 0.4 & 0.1 & 0.2 & 0.1 \\ 0.2 & 1 & 0.2 & 0.2 & 0.1 & 0.1 \\ 0.4 & 0.2 & 1 & 0.6 & 0.3 & 0.1 \\ 0.1 & 0.2 & 0.6 & 1 & 0.5 & 0.2 \\ 0.2 & 0.1 & 0.3 & 0.5 & 1 & 0.3 \\ 0.1 & 0.1 & 0.1 & 0.2 & 0.3 & 1 \end{bmatrix}$	25.2	58.6
19	43	42	38	38		34.7	44.9
22	33	33	30	30		18.5	22.1
25	20	22	26	26		15.1	17.6
33	29	30	34	36		12.4	26.0

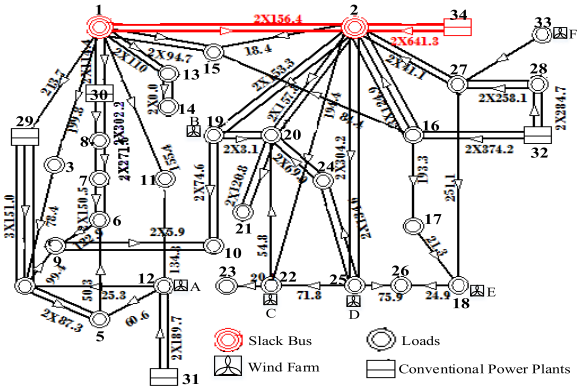

FIGURE 5. Configuration of the simplified real regional system.

TABLE 4. Comparisons of crude MC and the proposed IS in estimating probabilities of voltage violations and line overloads with and without frequency control in the real regional system.

	With Frequency Control			Without Frequency Control		
	$\hat{\mu}$	N^0_{CMC} / N^0_{IS}	r	$\hat{\mu}$	N^0_{CMC} / N^0_{IS}	r
V_{18}	5.8×10^{-4}	165600 / 740	224	5.2×10^{-4}	184700 / 800	230
V_{19}	4.9×10^{-4}	196000 / 810	242	3.3×10^{-4}	291000 / 900	323
V_{22}	7.9×10^{-5}	1215000 / 930	1306	4.6×10^{-5}	2087800 / 1380	1513
V_{20}	7.3×10^{-5}	1316600 / 940	1400	4.8×10^{-5}	2000800 / 1350	1482
$P_{19\text{-}20}$	3.3×10^{-4}	291030 / 720	404	2.1×10^{-5}	4573000 / 1780	2570
$P_{24\text{-}25}$	8.6×10^{-5}	1116700 / 800	1396	1.5×10^{-6}	64027000 / 4850	13200
$P_{22\text{-}25}$	8.2×10^{-5}	1171000 / 840	1394	-[a]	N/A	N/A
$P_{27\text{-}33}$	7.7×10^{-5}	1247000 / 890	1401	-[a]	N/A	N/A

[a] Values less than 10^{-6}

Center (JEPDC). The network configuration is depicted in Fig. 5 and it contains 3 voltage levels (500kV, 220kV and 33kV), 34 buses, 43 branches and 5 conventional power plants. Six wind farms are connected to buses 12, 18, 19, 22, 25 and 33 (marked A∼F) with nominal power of 55, 80, 100, 48, 50 and 42 MW, respectively. The IS schemes applied to the IEEE 14-bus test system only investigate the snapshot of operating conditions at time t_k. In real applications, security assessment should be performed at continuous time steps to capture any operating changes and identify the potential risks of the system. Suppose that the forecasts for wind and load used at t_k are from the historical data (10 a.m. July 1, 2016) at a resolution of 15 min ($\Delta t = 15$min). For the next time step $t_{k+1} = t_k + \Delta t$, the system load is expected to be increased by 6%. The parameters of wind forecasts at t_k and t_{k+1} are shown in table 3. Given that the time frame is short, the values of FOR provided by JEPDC at t_k and t_{k+1} are kept unchanged.

Table 4 lists the results of several bus voltages and line flows that have the highest risks. The speed-up of crude MC is even more pronounced here due to the low risk occurrence in the real systems. It is still true that a smaller probability can guarantee a larger speed-up ratio. An exception is for the case $\hat{\mu} = 8.2 \times 10^{-5}$ in P_{22-25}, where its ratio is less than that of the P_{24-25}. The discrepancy of the estimated $\hat{\mu}$ between the two scenarios is obvious even for the case of bus voltages. Since the probability of transmission line overload is relatively small when not considering the frequency regulation, only those lines with the probability higher than 10^{-6} are shown in the table (P_{19-20} and P_{24-25}). Therefore, the operating risks could be seriously underestimated, which demonstrates the necessity of incorporating the frequency performance into our model.

The relative error curves of the three IS schemes in estimating the probability of violating under-/over-regulation limits

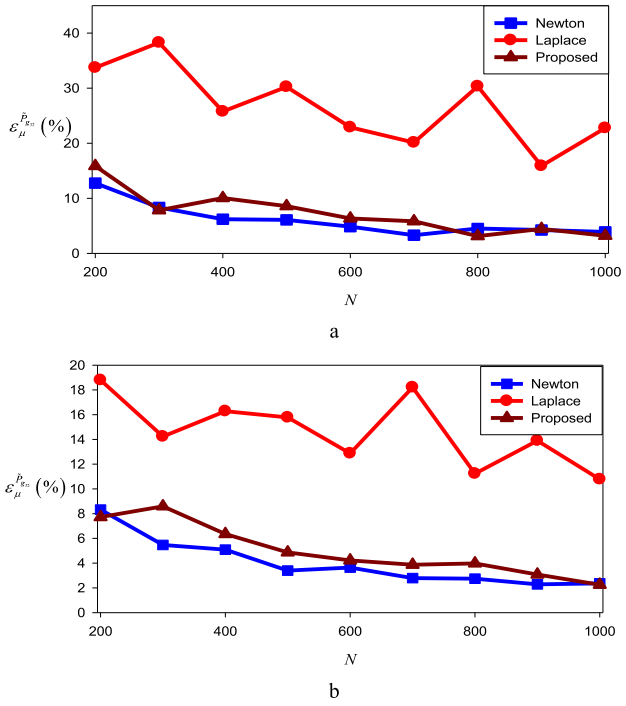

FIGURE 6. Error curve comparisons of P_{g32} by different IS schemes at time steps t_k and t_{k+1} in the real regional system: (a) t_k; (b) t_{k+1}.

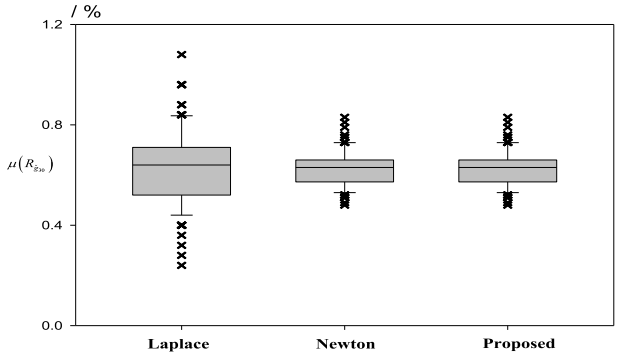

FIGURE 7. Boxplots of the ramping risk for g_{30} using different IS schemes.

of $g32$ are shown in Fig. 6 at time steps t_k and t_{k+1}, respectively. It can be seen that the Laplace has more than twice the error than the Newton and Proposed counterparts, and shows no sign of convergence within 1000 simulations. This means that the numerical robustness of the Laplace is very sensitive to the system dimension, hence it is not applicable when facing large complex networks. However, the Newton, which is outperformed by the other two IS schemes in the IEEE example, gives even more accurate results than those of the Proposed. Both of the methods converge after 800 simulations at the percentage error of nearly 2%.

Fig. 7 demonstrates the probability of violating the ramping constraints for generator $g30$ based on the 15-min forecasts (from t_k to t_{k+1}) via boxplots. The ramping rate of $g30$ in a specified time frame Δt is expressed as

$$\tilde{R}_{g_{30}} = \tilde{P}_{g_{30}}^{(t_{k+1})} - \tilde{P}_{g_{30}}^{(t_k)} / \Delta t \tag{32}$$

Clearly, we see a large variation of ramp-up/-down risk using the Laplace, whereas the results obtained by the Newton and Proposed concentrate in a small region near the median. This is consistent with the conclusion made as in Fig. 6 that the Newton and Proposed outperform the Laplace in larger systems with multiple variables.

VI. DISCUSSION & COMPARISON WITH PRIOR WORK

Comparing the problem formulation in Eq. (11) and (13) with the traditional one in Eq. (7), we can see that our characterization of the linearized PLF model is quite precise. To the best of our knowledge, this is the first time in the literature where the power flow analysis considering the steady-state behavior of the frequency regulation, the correlation and the large variation of input variables under various uncertainties is characterized in such a comprehensive manner. Specifically, the proposed model makes it possible to evaluate the probability of violating the generator ramping and over-/under-regulation limits by assuming that the power imbalance is charged to a group of dispatched generators instead of the single one at the slack bus. The results thus unfold a more real picture for the forecasted operating conditions and avoid underestimation of the system risk level under high renewable uncertainty.

Generally, most existing works for the power system security evaluation, using deterministic or probabilistic tools, are based on the $N-1$ or N-k criterion with a given operating condition. Tough the deterministically based approaches such as sensitivity analysis [29], have the merits of straightforward understanding and easy implementation, the results are highly conservative since it only depends on the worst-case scenario. For other works that are in the probabilistic framework, several reliability parameters like Loss of Load Probability (LOLP), Expected Energy Not Served (EENS) are used to reveal the effect of any cascading events [30]. However, such security metrics require extensive calculations to cope with the renewable uncertainty which presents at all times and is intrinsically different from rare contingency events. Hence, a highly desirable feature of the proposed security assessment is that it does not need to consider the situation after an $N-1$ outage and its potential cascading events. The risk indices are quantified in terms of the violation of technical limits, which are much easier to be calculated and for the system operators to identify the vulnerable or high-risk parts. Moreover, this type of risk measures are usually used for incorporation in the chance-constraint economic dispatch or unit commitment problems.

Finally, a newly designed IS estimator is proposed to fit the above PLF formulations for estimating the very low probability of the operating violations. Its numerical performance is tested and compared with other two commonly used IS schemes on two different-sized case studies. Though the level of error is very close to one another after 1000 samples, the proposed method shows better numerical stability for

a wide range of sample size and system dimensions. To achieve further reduction of the computational expense, other smart sampling strategies like Latin Hypercube sampling (LHS) and Quasi-Monte Carlo sampling (QMC) [31], can be adopted and combined with the proposed IS scheme to improve the sampling efficiency of the generalized random sampling method.

VII. CONCLUSION

This paper presents a stochastic framework in the assessment of power system security, accounting for uncertainties involving the contingencies and renewable energy forecasts. PLF, an efficient tool in probabilistic analysis, is modified to incorporate the steady-state behavior of the frequency regulation in the model which is represented as a piecewise affine approximation of the input power injections. The error induced by this linearized model is also alleviated using a multi-linearization procedure.

Particularly, an importance sampling technique adapted from mathematic finance is employed to speed-up the MCS in estimating the low-probability events. Two essential steps are modified to fit our applications: adjustments in the piecewise function of the state variables and design of the optimal IS distributions. Comparative studies and numerical experiments are carried out on both the IEEE 14-bus benchmark and a regional power network using the proposed method and other IS schemes. It shows that more accurate and robustness results are obtained simply by the proposed IS estimator with significant reduction of computational effort as compared to the crude MC.

It is noted that the probability indices computed in this paper only partially reveal the system security level in a steady-state manner. In this regard, future work should be done which accounts for the dynamic behavior of the system such as stability analysis, in order to form a comprehensive security domain where the proposed IS scheme can be applied to estimate the operating risks as well.

REFERENCES

[1] L. Roald, M. Vrakopoulou, F. Oldewurtel, and G. Andersson, "Risk-based optimal power flow with probabilistic guarantees," *Int. J. Elect. Power Energy Syst.*, vol. 72, pp. 66–74, Nov. 2015.

[2] J. C. Hernández, F. J. Ruiz-Rodriguez, and F. Jurado, "Modelling and assessment of the combined technical impact of electric vehicles and photovoltaic generation in radial distribution systems," *Energy*, vol. 141, pp. 316–332, Dec. 2017.

[3] M. Majidi-Qadikolai and R. Baldick, "Integration of $N-1$ contingency analysis with systematic transmission capacity expansion planning: ERCOT case study," *IEEE Trans. Power Syst.*, vol. 31, no. 3, pp. 2234–2245, May 2016.

[4] D. Devaraj and B. Yegnanarayana, "Genetic-algorithm-based optimal power flow for security enhancement," *IEE Proc.-Gener., Transmiss. Distrib.*, vol. 152, no. 6, pp. 899–905, Nov. 2005.

[5] Q. Wang, Y. Guan, and J. Wang, "A chance-constrained two-stage stochastic program for unit commitment with uncertain wind power output," *IEEE Trans. Power Syst.*, vol. 27, no. 1, pp. 206–215, Feb. 2012.

[6] X. Li, X. Zhang, L. Wu, P. Lu, and S. Zhang, "Transmission line overload risk assessment for power systems with wind and load-power generation correlation," *IEEE Trans. Smart Grid*, vol. 6, no. 3, pp. 1233–1242, May 2015.

[7] F. Bouffard and F. D. Galiana, "Stochastic security for operations planning with significant wind power generation," in *Proc. Power Energy Soc. Gen. Meeting-Convers. Del. Elect. Energy 21st Century*, Pittsburgh, PA, USA, 2008, pp. 1–11.

[8] Z. K. Wei, J. F. Xu, X. K. Dai, B. H. Zhang, S. L. Lu, and W. S. Deng, "Research on coarse-grained parallel algorithm of the Monte-Carlo simulation for probabilistic load flow calculation," in *Proc. Int. Conf. Power Energy (CPE)*, Shanghai, China, 2014, p. 77.

[9] R. N. Allan, A. M. L. da Silva, A. A. Abu-Nasser, and R. C. Burchett, "Discrete convolution in power system reliability," *IEEE Trans. Rel.*, vol. R-30, no. 5, pp. 452–456, Dec. 1981.

[10] M. A. Abdullah, A. P. Agalgaonkar, and K. M. Muttaqi, "Probabilistic load flow incorporating correlation between time-varying electricity demand and renewable power generation," *Renew. Energy*, vol. 55, pp. 532–543, Jul. 2013.

[11] G. Rubino and B. Tuffin, *Rare Event Simulation Using Monte Carlo Methods*. Rennes, France: Wiley, 2009.

[12] D. D. Le, A. Berizzi, and C. Bovo, "A probabilistic security assessment approach to power systems with integrated wind resources," *Renew. Energy*, vol. 85, pp. 114–123, Jan. 2016.

[13] H. Quan, D. Srinivasan, A. M. Khambadkone, and A. Khosravi, "A computational framework for uncertainty integration in stochastic unit commitment with intermittent renewable energy sources," *Appl. Energy*, vol. 152, pp. 71–82, Aug. 2015.

[14] H. Bludszuweit, J. A. Dominguez-Navarro, and A. Llombart, "Statistical analysis of wind power forecast error," *IEEE Trans. Power Syst.*, vol. 23, no. 3, pp. 983–991, Aug. 2008.

[15] S. Tewari, C. J. Geyer, and N. Mohan, "A statistical model for wind power forecast error and its application to the estimation of penalties in liberalized markets," *IEEE Trans. Power Syst.*, vol. 26, no. 4, pp. 2031–2039, Nov. 2011.

[16] P. Pinson, H. A. Nielsen, J. K. Møller, H. Madsen, and G. N. Kariniotakis, "Non-parametric probabilistic forecasts of wind power: Required properties and evaluation," *Wind Energy*, vol. 10, no. 6, pp. 497–516, 2007.

[17] Q. Xu, Y. Yang, Y. Liu, and X. Wang, "An improved latin hypercube sampling method to enhance numerical stability considering the correlation of input variables," *IEEE Access*, vol. 5, pp. 15197–15205, 2017.

[18] G. Sun, Y. Li, S. Chen, and H. Zang, "Dynamic stochastic optimal power flow of wind power and the electric vehicle integrated power system considering temporal-spatial characteristics," *J. Renew. Sustain. Energy*, vol. 8, no. 5, p. 053309, 2016.

[19] R. Wang, Y. Xie, H. Zhang, C. Li, and W. Li, "Dynamic power flow algorithm considering frequency regulation of wind power generators," *IET Renew. Power Gen.*, vol. 11, no. 8, pp. 1218–1225, 2017.

[20] D. Ke, C. Y. Chung, and Y. Sun, "A novel probabilistic optimal power flow model with uncertain wind power generation described by customized Gaussian mixture model," *IEEE Trans. Sustain. Energy*, vol. 7, no. 1, pp. 200–212, Jan. 2016.

[21] P. Zhang and S. T. Lee, "Probabilistic load flow computation using the method of combined cumulants and Gram-Charlier expansion," *IEEE Trans. Power Syst.*, vol. 19, no. 1, pp. 676–682, Feb. 2004.

[22] R. V. Hogg and A. T. Craig, *Introduction to Mathematical Statistics*, 5th ed. Upper Saddle River, NJ, USA: Prentice-Hall, 1995.

[23] P. Glasserman, W. Kang, and P. Shahabuddin, "Fast simulation of multifactor portfolio credit risk," *Oper. Res.*, vol. 56, no. 5, pp. 1200–1217, 2008.

[24] C. Hamon, M. Perninge, and L. Söder, "Efficient importance sampling technique for estimating operating risks in power systems with large amounts of wind power," in *Proc. 13th Wind Integr. Workshop*, London, U.K., 2014, pp. 22–24.

[25] D. Cai, D. Shi, and J. Chen, "Probabilistic load flow computation using copula and latin hypercube sampling," *IET Generat., Transmiss. Distrib.*, vol. 8, pp. 1539–1549, Jan. 2014.

[26] M. J. D. Powell, "A fast algorithm for nonlinearly constrained optimization calculations," in *Numerical Analysis* (Lecture Notes in Mathematics), vol. 630, G. A. Watson, Eds. Berlin, Germany: Springer, 1978, pp. 144–157.

[27] P. Glasserman, P. Heidelberger, and P. Shahabuddin, "Asymptotically optimal importance sampling and stratification for pricing path-dependent options," *Math. Finance*, vol. 9, no. 2, pp. 117–152, 1999.

[28] R. Christie. (1999). Power System Test Archive. University of Washington. Seattle, WA, USA. [Online]. Available: http://www.ee.washington.edu/research/pstca

[29] S. A. Farghal, M. A. Tantawy, A. A. A. Elela M. S. A. Hussien, and S. A. Hassan, "Fast technique for power system security assessment using sensitivity parameters of linear programming," *IEEE Trans. Power App. Syst.*, vol. PAS-103, no. 5, pp. 946–953, May 1984.
[30] Q. Wang, J.-P. Watson, and Y. Guan, "Two-stage robust optimization for N-k contingency-constrained unit commitment," *IEEE Trans. Power Syst.*, vol. 28, no. 3, pp. 2366–2375, Aug. 2013.
[31] Q. Xiao, "Comparing three methods for solving probabilistic optimal power flow," *Elect. Power Syst. Res.*, vol. 124, pp. 92–99, Jul. 2015.

YU HUANG received the B.S. degree in electrical engineering from the Nanjing University of Aeronautics and Astronautics, China, in 2015. He is currently pursuing the Ph.D. degree with the School of Electrical Engineering, Southeast University, China. He is also a Visiting Research Scholar with Purdue University, USA. His research interests include probabilistic load flow calculation, stochastic analysis and evaluation of renewable energy, and new energy power generation forecasting.

QINGSHAN XU (M'09) was born in China in 1979. He received the B.S. degree from Southeast University, China, in 2000, the M.S. degree from Hohai University in 2003, and the D.E. degree from Southeast University in 2006, all in electrical engineering. He was a Visiting Scholar and cooperates with the Aichi Institute of Technology, Japan, from 2007 to 2008. He is currently a Professor with the School of Electrical Engineering, Southeast University. His research interests include renewable energy and power system operation and control.

SAJJAD ABEDI (S'09–M'17) received the B.Sc. degree (Hons.) from the Isfahan University of Technology, Isfahan, Iran, the M.Sc. degree (Hons.) from the Amirkabir University of Technology (Tehran Polytechnic), Tehran, Iran, and the Ph.D. degree from Texas Tech University, Lubbock, TX, USA, in 2017, all in electrical engineering. He is currently a Post-Doctoral Research Fellow with the Department of Mathematics, School of Mechanical Engineering, Purdue University, West Lafayette, IN, USA. His research interests include power system modeling and operations, renewable energy integration, uncertainty and risk modeling, and predictive data analytics.

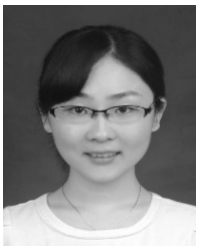

TONG ZHANG received the B.S. degree in electrical engineering from the Nanjing University of Aeronautics and Astronautics in 2015 and the M.S. degree in electrical engineering from the State Grid Electric Power Research Institute in 2018. She is currently a Researcher with the State Grid Jiangsu Electric Power Company Research Institute, China. Her research interests include power system monitoring and control.

XIANQIANG JIANG received the B.S. degree in electrical engineering from Shandong University, Jinan, China, in 2015. He is currently pursuing the M.S. degree in electrical engineering with Southeast University, Nanjing, China. His research interests include renewable energy and power system reliability.

GUANG LIN (M'12) received the B.S. degree in mechanics with a minor in electrical engineering from Zhejiang University, China, in 1997, the M.S. degree in mechanics and engineering science from Peking University, China, in 2000, and the M.S. and Ph.D. degrees in applied mathematics from Brown University, Providence, RI, USA, in 2004 and 2007, respectively.

He was a Senior Research Scientist with the Pacific Northwest National Laboratory in 2014. He is currently an Associate Professor with the Department of Mathematics, Purdue University. He has had in-depth involvement in developing uncertainty quantification tools for a large variety of domains including energy and environment. His research interests include diverse topics in computational science both on algorithms and applications, uncertainty quantification, large-scale data analysis, and multiscale modeling in a large variety of domains.

Dr. Lin is currently serving on the Editorial Board of the *International Journal for Uncertainty Quantification*.